JACS
JOURNAL OF THE AMERICAN CHEMICAL SOCIETY
Article
pubs.acs.org/JACS

On the Road from Formamide Ices to Nucleobases: IR-Spectroscopic Observation of a Direct Reaction between Cyano Radicals and Formamide in a High-Energy Impact Event

Martin Ferus,[†,‡] Svatopluk Civiš,*[,†] Arnošt Mládek,[§,∥] Jiří Šponer,[§,∥] Libor Juha,[‡] and Judit E. Šponer*[,§,∥]

[†]J. Heyrovský Institute of Physical Chemistry, Academy of Sciences of the Czech Republic, Dolejškova 3, CZ-182 23 Prague 8, Czech Republic

[‡]Institute of Physics, Academy of Sciences of the Czech Republic, Na Slovance 2, CZ-182 21 Prague 8, Czech Republic

[§]Institute of Biophysics, Academy of Sciences of the Czech Republic, Královopolská 135, CZ-612 65 Brno, Czech Republic

[∥]CEITEC-Central European Institute of Technology, Campus Bohunice, Kamenice 5, CZ-62500 Brno, Czech Republic

Supporting Information

ABSTRACT: The formamide-based synthesis of nucleic acids is considered as a nonaqueous scenario for the emergence of biomolecules from inorganic matter. In the current study, we scrutinized the chemical composition of formamide ices mixed with an FeNi meteorite material treated with laser-induced dielectric breakdown plasma created in nitrogen buffer gas. These experiments aimed to capture the first steps of those chemical transformations that may lead to the formation of nucleobases during the impact of an extraterrestrial icy body containing formamide on an early Earth atmosphere. High-resolution FT-IR spectroscopy combined with quantum chemical calculations was used to analyze the volatile fraction of the products formed during such an event. We have found that the spectrum of the evaporated formamide ices is dominated by the spectral signatures of the dimeric form of formamide. Upon exposure to laser sparks, new well-defined bands appear in the spectrum centered at ~820, ~995, and ~1650 cm^{-1}. On the basis of quantum chemical calculations, these bands can be assigned to the absorptions of 2-amino-2-hydroxy-acetonitrile and to 2-amino-2-hydroxy-malononitrile, which are formed in a direct reaction between formamide and $CN^{\bullet}$ radicals upon the high-energy impact event. We also show that there is an exergonic reaction route via these intermediates leading to diaminomaleonitrile, which is generally considered to play a key role in the synthesis of nucleobases.

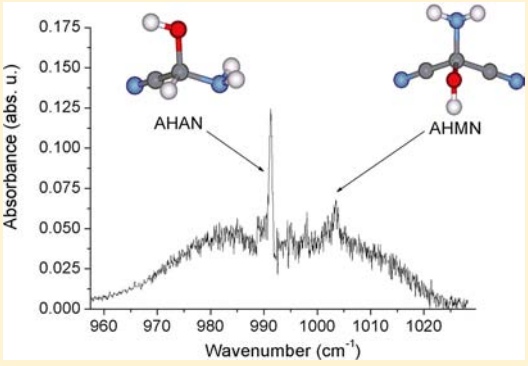

INTRODUCTION

The formamide-based synthesis of nucleobases was elaborated as a nonaqueous variant for the origin of life. Formamide represents the simplest form of peptide linkage, and as it is the hydrolysis product of HCN, it is quite abundant in space. It has been detected in interstellar ices[1] and comets,[2] and on the basis of its high availability, this molecule has been suggested as a possible extraterrestrial parent of biomolecules.

Saladino and co-workers demonstrated that formamide can be converted to all five nucleobases with a relatively good yield using various catalysts. In the presence of clay catalysts, the Saladino synthesis forms cytosine and uracil[3] in addition to the main products purine[4] and adenine,[5] while the main product is thymine[6] when TiO_2 is used as a catalyst. Formation of hypoxanthine and guanine has been reported over pyrophosphates.[7] Moreover, Strecker condensation of formamide with HCN (which is the dissociation product of formamide) leads to the formation of amino acids.[8]

In our previous computational paper,[9] on the basis of experimental proposals from ref 3 we presented a plausible reaction pathway for the Saladino synthesis and noted that the cyclization reaction step leading to the formation of the pyrimidine ring requires considerably higher activation energy than any of the corresponding aqueous synthetic methods. The high activation energy explains why relatively harsh reaction conditions are utilized in the Saladino synthesis. Nonetheless, our computations reveal that the reaction path suggested by Saladino et al. is feasible in the temperature range at which formamide is a liquid.

A rather elegant manner to overcome problems related to the high activation energy is to use high-energy photons to initiate the chemical processes. An example of this has already been reported by Barks et al.,[10] who studied nucleobase formation by irradiating formamide solutions with UV light. Nonetheless, in this study the authors point out that nucleobases are formed exclusively in those cases when irradiation is associated with heating. In ref 11. Saladino and co-workers have studied polymerization of formamide in the presence of TiO_2 catalyst and under an exposure to synchrotron light. Surprisingly,

Received: October 22, 2012
Published: November 30, 2012

   dx.doi.org/10.1021/ja310421z | J. Am. Chem. Soc. 2012, 134, 20788−20796

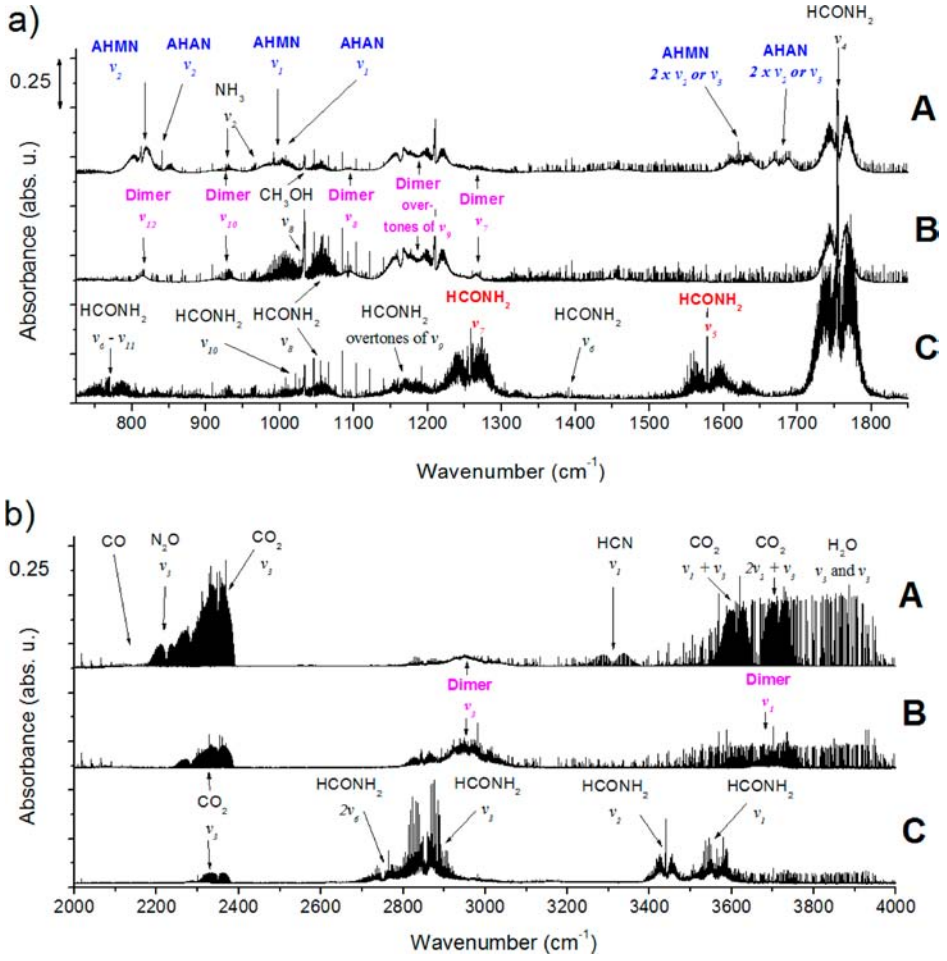

Figure 1. Comparison of the vapor phase spectra of liquid formamide and its ice in the MIR (a) and NIR (b) spectral ranges. The spectrum of the irradiated, and subsequently melted, formamide ice mixed with a FeNi meteorite is depicted in panel A. The broad bands of the products AHAN and AHMN are marked in blue. This spectrum is compared with that recorded for the gas phase of melted, nonirradiated pure formamide ice in panel B. The bands of the formamide dimer are marked in violet. The spectrum of the pure formamide vapor is depicted in panel C. The missing bands ν_7 (CN stretching) and ν_5 (NH_2 scissoring) of formamide are marked in red.

instead of nucleobases, they have observed formation of carboxylic acid intermediates of the Krebs cycle. Thus, currently the photochemical route to the formation of nucleobases is a subject of debate.

Plasma formed during the impact of an extraterrestrial body with an atmosphere offers another solution for problems related to the high energy barrier of chemical reactions. In our former study, we focused on the chemical transformations[12] that occur in a laser-induced dielectric breakdown (LIDB) plasma and on the subsequent reactions of the decomposition products,[13−15] which eventually lead to biomolecules (nucleobases and amino acids[16]). LIDB in the gas phase serves as a model of a hot and dense plasma generated by the impact of an extraterrestrial body on planetary atmospheres, and formamide ice mixed with the FeNi meteorite material simulates an extraterrestrial icy impactor. In the LIDB plasma, all the characteristics of a high-energy density event manifest themselves: the shock raises the temperature[17] to several thousand kelvin, which is accompanied by the formation of a shock wave and the generation of secondary hard radiation (UV−VUV, XUV, and X-ray). In our previous study we identified the main formamide decomposition products (HCN, CO_2, CH_3OH, CO, and NH_3) in the gas phase.[18] We have also simulated the decomposition processes at a plasma temperature of 4500 K by a chemical model. Additionally, the time-resolved emission spectroscopy of a glow discharge[19] has been used to study the unstable products of formamide decomposition, such as the HNC molecule or the reactive $CN^{\bullet}$ radical.[20]

In the current study, we use IR spectroscopy combined with quantum chemical calculations to investigate the product composition of formamide ices treated with laser sparks. In particular, we concentrate on the volatile fraction of the products, i.e., those compounds that can be detected upon evaporation of the formamide ices at room temperature.

To identify the spectra of these species, we use quantum chemical calculations. The great advantage of this methodology is that it is able to provide a simultaneous picture of molecular structure, energy, and spectroscopic properties. The method was found to be useful in the past when addressing various problems related to the origin of life.[21−30] Beyond the spectral analysis, we also suggest a possible mechanistic scenario for the formation of those simple molecules that may be involved in the formamide-based synthesis of nucleobases in a high-energy density impact event.

■ EXPERIMENTAL SECTION

FT-IR spectroscopy was used for the high-resolution detection of the absorption bands of molecules and molecular clusters in the gas phase.

dx.doi.org/10.1021/ja310421z | J. Am. Chem. Soc. 2012, 134, 20788−20796

Table 1. Vibrational Wavenumbers (cm^{-1}) and Relative Intensities (in percentages of that of the strongest absorption) of the Monomeric and H-Bonded Dimeric Forms of Formamide, From Experiment and Computations

	monomer							dimer				
	exptl			comptd				exptl		comptd		
	freq		int	freq	freq [a] this study		int	freq	int	freq		int
vibration	ref 37	this study[a]	this study[a]	ref 43[b]	unscaled	scaled[c]	this study[a]	this study[a]	this study[a]	this study[a] unscaled	scaled[c]	this study[a]
NH_2 out of plane deformation "wagging", ν_{12}	289			243	162	157	49.0			482	463	16.7
										485	466	1.8
								814	1 (0.01)[d]	823	790	0
										871	836	5.0
out of phase NH_2/NCO bend "rocking", ν_9	566			558	557	535	2.4			601	577	0
NH_2 out of plane deformation "twisting", ν_{11}	602			620	641	615	3.4			620	595	1.1
H−C out of plane deformation, ν_{10}	1033	1021	9 (0.10)	1015	1036	995	1.7	923	2 (0.04)	1053	1011	0
										1065	1022	2.2
in phase NH_2/NCO bend "rocking", ν_8	1046	1045	5(0.06)	1031	1052	1010	1.0	1075	9 (0.18)	1089	1046	0
										1094	1051	0
C−N stretching, ν_7	1258	1258	58 (0.68)	1234	1266	1215	25.9	1266	2 (0.04)	1334	1281	12.3
										1353	1299	0
H−C in plane bending "scissoring", ν_6	1391	1391	1 (0.02)	1384	1405	1349	0.9	1452	7 (0.14)	1409	1353	3.3
										1411	1355	0
H−N−H in plane bending "scissoring", ν_5	1579	1577	36 (0.30)	1579	1619	1555	9.6			1618	1554	0
										1641	1576	1.0
C═O stretching, ν_4	1754	1754	100 (1.16)	1738	1763	1693	100.0			1743	1673	0
								1755	100 (1.98)	1759	1689	66.7
C−H stretching, ν_3	2854	2851	43 (0.50)	2861	3034	2914	19.0	2947	13 (0.25)	3057	2936	17.9
										3059	2937	0
N−H symmetric stretching, ν_2	3440	3440	43 (0.50)	3482	3603	3461	11.6			3318	3187	0
										3349	3216	100
N−H antisymm. stretching, ν_1	3564	3563	43 (0.50)	3612	3763	3614	12.7	3681	2 (0.04)	3707	3560	14.7
										3708	3561	2.3
large amplitude dimer modes										61	59	1.9
										136	131	0
										150	144	3.1
										174	167	0
										218	209	0
										220	211	7.2

[a]Computed at the MP2/aug-cc-pVDZ level of theory. [b]Frequencies in ref 43 were computed at the B3LYP/CBS (CBS = complete basis set) level. [c]A scaling factor of 0.9604 was used to calculate the scaled vibrational frequencies. [d]Numbers in parentheses refer to the experimentally measured absorption intensities in absorption units.

Measurement was performed using a Bruker IFS 125 HR spectrometer equipped with semiconductor MCT (HgCdTe) and InSb nitrogen-cooled detectors in the ranges of 680−3500 cm^{-1} and 1800−5500 cm^{-1}, respectively. A resolution of 0.02 cm^{-1} was used as a reasonable compromise considering the signal/noise ratio, the duration of the measurement using 300 scans, and a multipass cell with an optical path of 30 m.

The formamide samples (Sigma Aldrich, molecular biology grade ≥99.5%) were frozen at 77 K and exposed to periodic laser impulses (15 pulses every 20 min) generated by the high performance PALS system[31] (wavelength of 1315 nm, energy of 150 J, and a duration of 350 ps). This experiment was performed in the presence of millimeter-sized particles of the FeNi meteorite *Campo del Cielo*[32] and nitrogen (Linde Gas, 99.9999%) as a buffer gas. The formamide sample was saturated with nitrogen gas and subsequently frozen with liquid nitrogen. The saturation process was controlled by following the drop of vapor pressure in the liquid−vapor equilibrium system. After irradiating the sample, the buffer gas was removed, and the sample was allowed to melt and reach room temperature.

Additionally, the samples of formamide ices mixed with HCN, HNCO, and NH_3 were prepared for comparative spectroscopic measurements. Liquid formamide was mixed with the gas phase of these compounds and subsequently frozen by liquid nitrogen. Before measurement, all the ices (i.e., comparative samples and irradiated formamide) were melted, and the multipass cell was filled with the gas sample.

COMPUTATIONAL SECTION

Mechanism of the Diaminomaleonitrile Formation. Geometries were optimized at the B3LYP/6-311++G(2d,2p) level of theory with relaxation of all structural parameters. (Cartesian coordinates of all optimized geometries are listed in the Supporting Information.) Free energies of the studied compounds (G) were calculated from the total electronic energy (E^{tot}) and from the thermal and entropic correction terms to the Gibbs free energy (δG) via harmonic approximation from frequency calculations:

$$G = E^{tot} + \delta G \quad (1)$$

dx.doi.org/10.1021/ja310421z | J. Am. Chem. Soc. 2012, 134, 20788−20796

In addition, we have carried out a set of benchmark calculations at the CCSD(T)/6-311++G(2d,2p) level using the B3LYP/6-311++G(2d,2p) optimized geometries. In this case free energies were computed using the electronic energies from CCSD(T)/6-311++G(2d,2p) single point calculations as well as the δG term derived from B3LYP/6-311++G(2d,2p) calculations.

All calculations were carried out in the gas phase using the G03 program package.[33]

Calculations of Vibrational Spectra. Vibrational wavenumbers used for interpretation of the experimentally measured spectra were computed at the MP2/aug-cc-pVDZ level of theory using optimized geometries computed in the gas phase at the same theoretical level in the harmonic approximation. The Resolution of Identity (RI) approximation[34,35] and the Turbomole 6.3 program package[36] were used throughout these calculations.

RESULTS AND DISCUSSION

1. Infrared Spectra. First of all, absorption bands of typical formamide dissociation products (HCN, NH_3, CO, N_2O, H_2O, CO_2, and CH_3OH)[18] have been identified in the gas phase spectra from melted formamide ice irradiated in the presence of millimeter-sized FeNi meteorite particles. The middle infrared (MIR) region of the spectrum is shown in Figure 1a, panel A, and the near-infrared (NIR) region of the same spectrum is shown in Figure 1b, panel A. In addition to the bands of the simple molecular dissociation products mentioned above, we have also found several new bands. For comparison, we have also recorded the gas phase infrared spectrum of melted formamide ice as well as that of liquid formamide not treated with laser impulses. These spectra are presented in parts a and b of Figure 1, panels B and C, respectively.

The gas phase spectrum of the volatile part of the formamide liquid sample (panel C in Figure 1) is highly reminiscent of the spectrum reported in ref 37 (for a comparison of the band positions measured in this work and in ref 37, see columns 1−2 of Table 1) and is strikingly different from the spectra of formamide ices presented in panels A and B of Figure 1. To identify the rovibrational bands observed in the gas phase spectra of melted formamide ices (with and without irradiation), we have carried out a set of quantum chemical calculations with the aim to assess the vibrational spectra of several species that might be formed in the reaction mixture.

2. Interpretation of the Infrared Spectra. *2.1. Computed Vibrational Frequencies of the Monomeric and Dimeric Forms of Formamide.* Several studies have been devoted to the experimental[37,38] and theoretical[39−44] investigation of the vibrational spectrum of monomeric formamide in the gas phase. Our computed vibrational wavenumbers are compared to the most recent available literature data[37,43] in Table 1 columns 4−6. In addition to the computed MP2/aug-cc-pVDZ wavenumbers, Table 1 also lists the scaled vibrational wavenumbers derived from the computed ones using a scaling factor of 0.9604, as suggested by Sinha et al.[45] Surprisingly, scaling improves the agreement with the experimental data only for wavenumbers above 3000 cm^{-1}. In the 800−2000 cm^{-1} interval, the unscaled values fit the experimental data better than the scaled ones. Because the most remarkable differences between the spectra shown in panels A, B, and C of Figure 1 are in the 800−2000 cm^{-1} interval (and, in addition, this spectral region is not disturbed by bands arising from the absorptions of the various dissociation products of formamide), all our spectral interpretations are based on the unscaled vibrational wavenumbers hereafter.

2.2. Interpretation of Formamide Gas Phase Spectrum. The gas phase spectrum of formamide (resolution 0.02 cm^{-1}) is depicted in parts a and b of Figure 1, panel C. In general, this spectrum is consistent with the one measured by McNaughton et al.[37] The rovibrational band centered at 1754 cm^{-1} can be assigned to the C═O stretching mode (denoted as ν_4 in ref 37) of formamide. The broad absorption centered at 1577 cm^{-1} corresponds to the in-plane NH_2 scissoring vibrational mode of formamide (ν_5); the intensity thereof, in line with our computations, is approximately an order of magnitude lower than that of the ν_4 mode observed at 1754 cm^{-1}. The rovibrational band centered at 1258 cm^{-1} is consistent with the ν_7 CN stretching mode of formamide. This is supported not only by the position of the band but also by its intensity, which might be about 25% of that of the main ν_4 absorption observed at 1754 cm^{-1}, according to our computations. The broad and significantly less intense rovibrational band centered at 1160 ± 50 cm^{-1} incorporates several weaker absorptions, among them the first overtone of the ν_9 vibration ($2\nu_9$, 2 × 566 = 1132 cm^{-1}), as well as the sum of the ν_9 and ν_{11} absorptions (ν_9 + ν_{11}, 565 + 602 = 1167 cm^{-1}).[37] Another broad and weak band can be observed at 1040 ± 30 cm^{-1} that can be assigned to an in-phase NCO/NH_2 bending mode (ν_8, 1045 cm^{-1}) and to the out of phase C−H deformation (ν_{10}, 1021 cm^{-1}). In addition, we have observed three weak, yet well-defined, bands centered at ∼970, ∼930, and 770 cm^{-1}. Because these bands were not observed in the spectrum reported by McNaughton et al.,[37] they can likely be assigned to molecules other than formamide.

2.3. Gas Phase Spectrum of Melted Formamide Ice. The most significant change observed after freezing out the formamide samples is the complete absence of the dominant ν_5 absorption band centered at 1577 cm^{-1} and the dramatic reduction and slight blue-shift of the ν_7 absorption from 1258 to 1266 cm^{-1} (see Figure 1a, panel C, with the positions of the missing bands marked in red). Thus, freezing out the samples primarily affects the wavenumber of the in-plane NH_2 scissoring (ν_5) and CN stretching (ν_7) modes. This result is compatible with the formation of a cyclic formamide dimer shown in Figure 2a.

Notably, the cyclic structure, which is stabilized by two H-bonds, is the most stable configuration of the formamide dimer. Numerous prior computations have shown that the binding energy of this configuration is approximately 5 kcal/mol higher (in absolute value) than those of the other four isomers and therefore represents the dominant dimer species in the vapor phase,[41,42,46,47] if any dimer is formed.

Because our computed frequency data obtained for the monomeric form of formamide at the MP2/aug-cc-pVDZ level have shown a good qualitative agreement with high level (B3LYP/CBS level) computational and experimentally measured data, we used the same theoretical approach to compute the vibrational wavenumbers and intensities for the cyclic formamide dimer. When comparing the frequency and intensity data of the dimer to the corresponding monomer data (see Table 1), the relative intensity of the ν_5 mode of the dimer (2% of the main ν_4 absorption) is substantially reduced compared to that of the monomer (26% of the main ν_4 absorption). The same behavior was also observed in our spectrum recorded after freezing out the samples (see panel B in Figure 1) because no absorption band was observed in the spectral region of 1550−1700 cm^{-1}. Weakening of the ν_7 absorption at 1255 cm^{-1} can also be explained by the formation of cyclic dimers. According

dx.doi.org/10.1021/ja310421z | J. Am. Chem. Soc. 2012, 134, 20788−20796

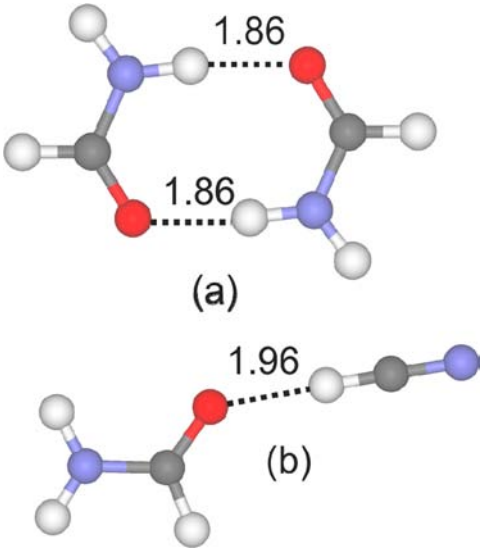

Figure 2. MP2/aug-cc-pVDZ optimized geometries of (a) the most stable isomer of formamide dimer and (b) the formamide···HCN complex considered in the frequency calculations. Numbers next to the dotted lines are the lengths of the H-bonding contacts in angstroms.

to our calculations, upon dimer formation the position of the ν_7 band should be blue-shifted by ~60 cm^{-1}, with a concomitant reduction of its relative intensity compared to that of the monomer. Indeed, in the dimer spectrum the significantly reduced ν_7 absorption is located 11 cm^{-1} higher than the corresponding band of the monomer at 1266 cm^{-1}.

2.4. Gas Phase Spectrum of LIDB Treated Formamide Ice Mixed with FeNi Meteorite. The gas phase spectrum of the LIDB treated formamide ice mixed with FeNi meteorite, apart from showing the main characteristics of the cyclic dimer, exhibits four additional broad absorptions in the range of 1600−1700 cm^{-1}. In addition, well-defined bands appear centered at ~820, ~995, and ~1650 cm^{-1}. A detailed view of the fine structure of the new bands is presented in Figure 3.

Because a large amount of free HCN was observed in the reaction mixture, we tried to assign the band at 820 cm^{-1} to the characteristic H−C out of plane bending vibrations present either in the HCN dimer or in a formamide···HCN complex. Our computed MP2/aug-cc-pVDZ wavenumbers for the corresponding vibration in a formamide···HCN complex (Figure 2b) are 865 and 873 cm^{-1}. The computed intensity of these two absorptions is in total 13% of that of the main ν_4 absorption band (i.e., the C═O stretching mode of formamide). The band centered at 820 cm^{-1} can be attributed to a HCN dimer as well. MP3/6-311++G(2d,2p) level calculations propose the existence of a band centered at 845 cm^{-1} (the intensity thereof is 24% of the main absorption), which can be associated with the C−H deformation vibration of the HCN dimer.[48] This assignment could also provide an alternative interpretation for the origin of the newly formed broad absorption bands in the range of 1600−1700 cm^{-1}, which might be the first overtones of the H−C out of plane bending vibrations either in the HCN dimer or in the HCN···formamide complex. To verify our theoretical assignment, we measured the spectrum of melted formamide ices that were saturated with HCN. New bands were not detected in these spectra except those that were assigned to monomeric and dimeric forms of the formamide dimer, formamide vapor,

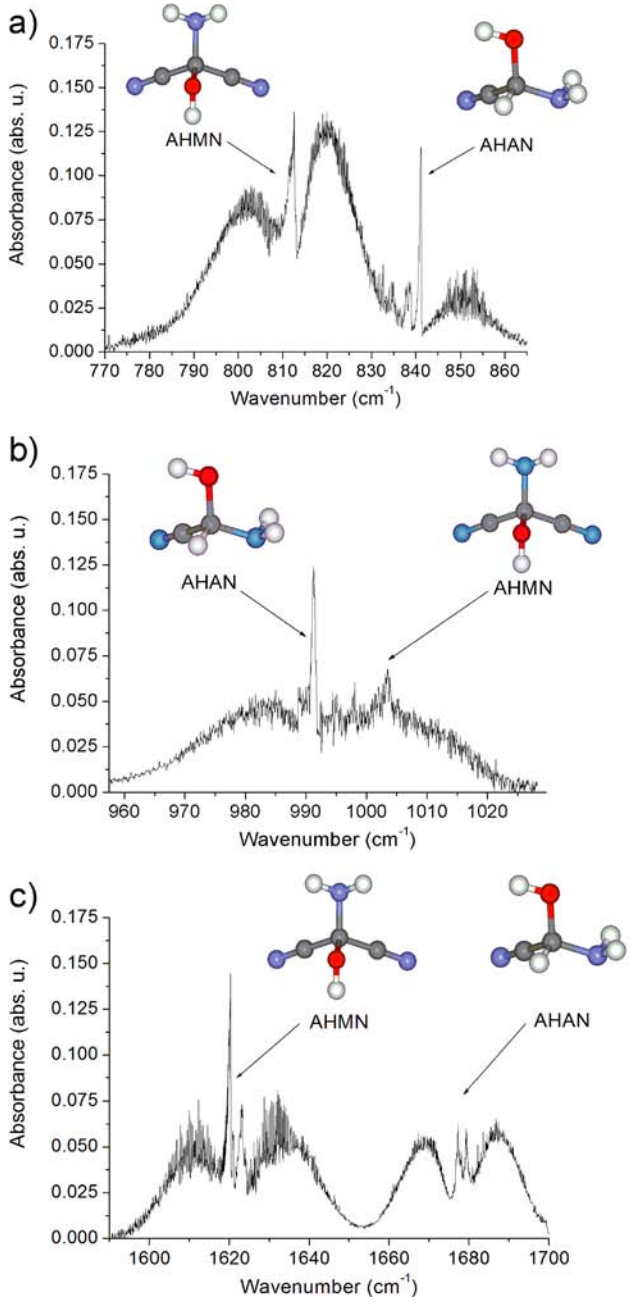

Figure 3. Detailed view of the 2-amino-2-hydroxy-acetonitrile (AHAN) and 2-amino-2-hydroxy-malononitrile (AHMN) bands in the spectra of the high power laser irradiated ices. All the modes can be found in the MIR region of spectra. (a) The NH_2 deformation mode is situated at ~820 cm^{-1}, (b) the CO stretching mode at ~995 cm^{-1}, and (c) the second harmonic of the NH_2 deformation at 1650 cm^{-1}. The lines of other molecules absorbing in the same range have been eliminated from the spectra.

and HCN. Additionally, analogous experiments have been performed with formamide−NH_3 and formamide−HNCO ices with the same results: the new bands mentioned above were not detected. This observation rules out that the 820 cm^{-1} band is due to complex formation with HCN.

In addition, complexation with HCN would not explain the origin of the absorption at ~995 cm^{-1}. Because this band is not present in any other spectra that we measured, we thought that it might be strongly associated with the photochemical reactions initiated by exposure to laser sparks. For this purpose,

dx.doi.org/10.1021/ja310421z | J. Am. Chem. Soc. 2012, 134, 20788−20796

we have computed the vibrational wavenumbers for 2-amino-2-hydroxy-acetonitrile (hereafter abbreviated as AHAN; see Scheme 1), which is the product of the addition reaction

Scheme 1

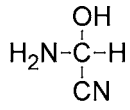

2-amino-2-hydroxy-acetonitrile
(AHAN)

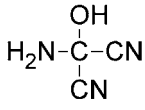

2-amino-2-hydroxy-malononitrile
(AHMN)

between a CN• radical and formamide.[49] This compound may be formed as a byproduct of the stepwise reaction leading from formamide to 2,3-diaminomaleonitrile (DAMN, *vide infra*), which has been suggested to be an important precursor of purine bases in a photochemically activated formamide-based prebiotic synthesis of nucleobases.[10,50] Indeed, we have found that the most intense band in the theoretical MP2/aug-cc-pVDZ spectrum of AHAN (depicted in Figure 4) is at 1021 cm^{-1}, associated with a C−O stretching vibration (hereafter classified as ν_1) with some contribution from the deformation of the amino group.[51] On the basis of our computations, the second most intense band (hereafter labeled as ν_2) produced by AHAN in the spectral region studied by us belongs to an NH_2 deformation and is centered at 847 cm^{-1}. In addition, the theoretical spectrum of AHAN displays a band of medium intensity located at 1652 cm^{-1}, which can be assigned to an H−N−H bending vibration (ν_3).

Viewing the theoretical spectrum of 2-amino-2-hydroxy-malononitrile (AHMN, see Scheme 1 and Figure 4) may provide an alternative interpretation for the origin of the bands at ∼820, ∼995, and ∼1655 cm^{-1}. This compound can be deduced from AHAN by substituting a CN group for its H connected to C2. The spectrum is featured basically by the same vibrations as that of AHMN, albeit with slightly shifted band positions. A comparison of the positions of the ν_1−ν_3 bands of AHAN and AHMN along with their intensities and the experimentally measured band positions is presented in Table 2. The computed MP2/aug-cc-pVDZ vibrational spectrum of AHMN, similar to that of AHAN, is dominated by a band centered at 1035 cm^{-1} assigned to a C−O stretching vibration combined with the deformation of the amino group. This puts forward another plausible assignment for the experimentally measured absorption at ∼995 cm^{-1}. Apart from the main ν_1 absorption, our computations predict another rather strong band for this compound (with an intensity of 62% of the main absorption) centered at 833 cm^{-1} due to an NH_2 deformation vibration (ν_2), which is consistent with the experimentally observed band at ∼820 cm^{-1}. In addition, another NH_2 deformation (ν_3) should appear at 1646 cm^{-1}, with an intensity of ∼19% of the main absorption. This may explain the origin of one of the weak absorption bands

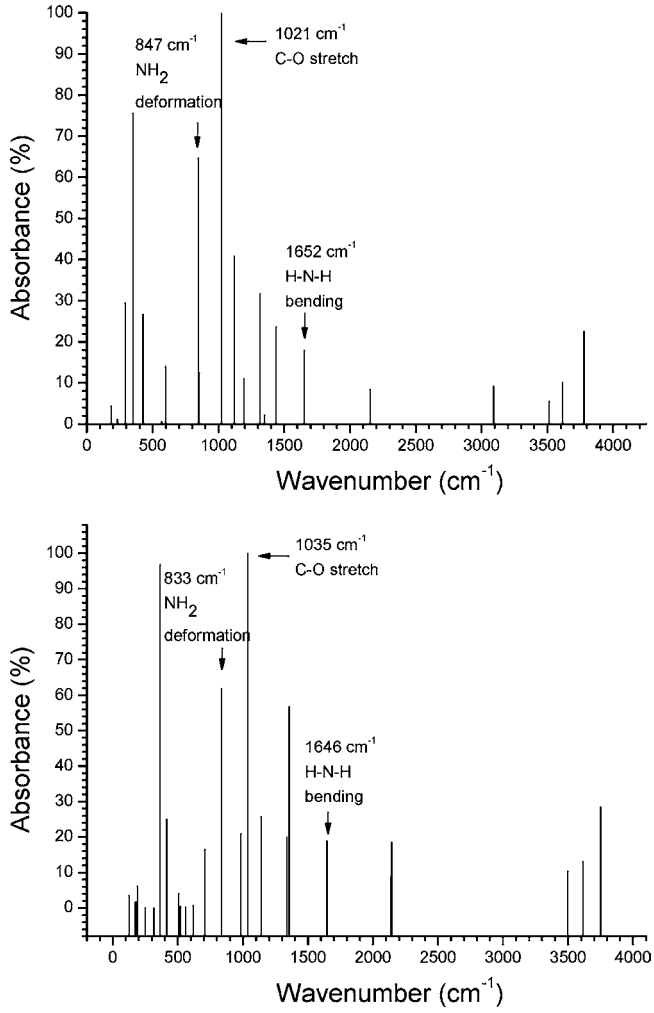

Figure 4. MP2/aug-cc-pVDZ computed spectra of 2-amino-2-hydroxy-acetonitrile (AHAN, upper) and 2-amino-2-hydroxy-malononitrile (AHMN, bottom).

observed in the ∼1655 cm^{-1} spectral region. Let us note that based on our computations the ν_3 bands of AHAN and AHMN may appear at very similar wavenumbers as $2\nu_2$, which makes assignment of the absorptions at ∼1655 cm^{-1} ambiguous.

2.5. Reaction Route to 2,3-Diaminomaleonitrile from Formamide and HCN. 2,3-Diaminomaleonitrile was found to be an intermediate of the photochemically activated formamide-based nucleobase synthesis.[10] Using quantum chemical calculations, we attempted to describe the reaction route leading from formamide to this compound, assuming that the reaction mixture contains a large amount of CN• radicals, which are formed as a dissociation product of formamide.[18] The elementary steps and the free energy profile of the reaction are summarized in Figure 5. The first reaction step involves addition of a CN• radical to the C═O double bond, which requires an activation energy of 11.2 kcal/mol and is weakly exothermic: the reaction free energy change, hereafter abbreviated as ΔG_{react}, is −7.4 kcal/mol (B3LYP/6-311++G(2d,2p) level). The radical product of the first reaction step may be stabilized via spontaneous H-loss in the second reaction step, resulting in the formation of 1-cyanoformamide. A byproduct of this reaction step could also be AHAN, which may be readily formed as the recombination product of the adduct formed by formamide and a CN• radical with an H

dx.doi.org/10.1021/ja310421z | J. Am. Chem. Soc. 2012, 134, 20788−20796

Table 2. Comparison of the Computed MP2/aug-cc-pVDZ Vibrational Wavenumbers (cm^{-1}) and Intensities (in percentage of the strongest absorption) of 2-Amino-2-hydroxy-acetonitrile (AHAN, see Scheme 1) and 2-Amino-2-hydroxy-malononitrile (AHMN, see Scheme 1) with the Experimentally Determined Positions of the New Bands Measured for the Products Formed upon Irradiation with a High Power Laser

	comptd				exptl	
	AHAN		AHMN			
asgnmt	freq	int	freq	int	freq	int[a]
C−O stretch, ν_1	1021	100	1035	100	991	92 (0.12)
					1003	54 (0.07)
NH_2 deformation, ν_2	847	65	833	62	812	100 (0.13)
					841	85 (0.11)
$2\nu_2$	1694		1666		1669	77 (0.10)
					1688	62 (0.08)
H−N−H bending, ν_3	1652	18	1646	19		

[a]Absolute values in absorbance units are given in parentheses.

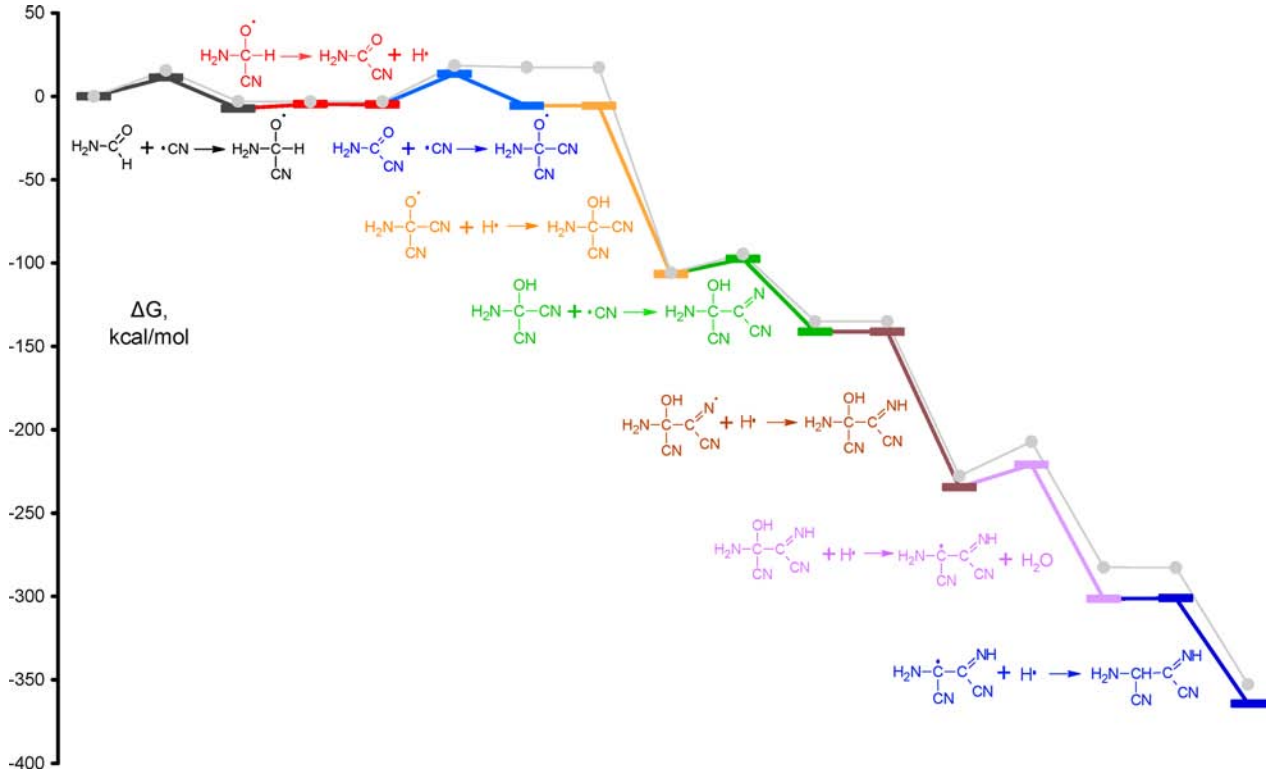

Figure 5. Energy profile of the formation of 2,3-diaminomaleonitrile from the reaction of formamide with CN• radicals. The individual reaction steps are highlighted with different colors on the curve computed at the B3LYP/6-311++G(2d,2p) level. The gray curve presents the CCSD(T)/6-311++G(2d,2p) benchmark energy data using the B3LYP/6-311++G(2d,2p) optimized geometries.

atom. In the third reaction step, an additional CN• radical is added to the 1-cyanoformamide. This reaction step is weakly exothermic (ΔG_{react} = −0.7 kcal/mol) and requires a relatively low activation energy of 18.3 kcal/mol. In the fourth reaction step, the radical product of the cyanide addition stabilizes as AHMN in an energetically downhill, markedly exothermic reaction step (ΔG_{react} = −101.0 kcal/mol). It is important to note that the spectral signatures of AHMN have also been detected in our spectra. This is followed by the addition of a CN• radical to one of the cyano groups of 2-amino-2-hydroxy-malononitrile, again in a strongly exothermic step (ΔG_{react} = −35.6 kcal/mol), which proceeds with a very low activation energy of 8.9 kcal/mol. In the sixth step, similar to the fourth, the product radical of the fifth step recombines with an atomic H, which is an energetically downhill step that leads to the formation of 2-amino-2-hydroxy-3-imino-succinonitrile. In the next reaction step, this molecule loses the 1-hydroxyl group in a reaction with atomic H in a notably exothermic reaction step (ΔG_{react} = −67.0 kcal/mol) that requires an activation energy of 13.5 kcal/mol. In the last step, the radical product of the previous step recombines with an atomic H, resulting in the formation of the amino−imino tautomeric form of DAMN. In total, the whole reaction path is markedly exothermic. The CN• radical behaves in the reaction as an energy reservoir because conversion of its triple bond to a single C−N bond is accompanied with the release of a large amount of binding energy. Moreover, this open shell radical is characterized by many excited electronic and vibrational−rotational states. This could provide a tremendous driving force for chemical transformations in the universe.

dx.doi.org/10.1021/ja310421z | J. Am. Chem. Soc. 2012, 134, 20788−20796

The relevance of this reaction pathway is exemplified with the good agreement between the experimentally measured absorptions of formamide samples treated with high-energy laser pulses and the computed vibrational spectra of two intermediates, i.e., AHMN and AHAN.

Because all of the reaction steps have relatively low activation energies (<20 kcal/mol), one would expect that no catalyst is needed to facilitate the elementary processes. In spite of this, the formation of AHAN and AHMN was not observed without the use of the FeNi meteoritic material. The reason for this could be that the cross section of the reaction is relatively low in the cooling plasma due to the low concentration of the $CN^{\bullet}$ radicals. The meteoritic material exerts its catalytic effect via binding and concentrating the $CN^{\bullet}$ radicals, which may lead to significant enhancement of the reaction rates.

CONCLUSIONS

In the current paper we have used a combined experimental–theoretical approach to investigate the composition of formamide ices mixed with FeNi meteorite after LIDB exposure. This system can be considered as a mimic of an impact of an icy extraterrestrial body containing formamide on a planetary atmosphere. We have focused on the volatile fraction of the products, which have been analyzed using high-resolution IR spectroscopy.

The typical products of formamide decomposition (HCN, NH_3, CO, N_2O, H_2O, CO_2, and CH_3OH) have been identified in the spectra together with the dimeric form of formamide. Additionally, for the first time, we have succeeded in identifying the spectral signatures of two reaction products formed from the direct reaction between formamide and $CN^{\bullet}$ radicals: 2-amino-2-hydroxy-acetonitrile (AHAN) and 2-amino-2-hydroxy-malononitrile (AHMN). However, these compounds were detected only in the presence of an FeNi meteoritic material.

In general, our findings support the view of Barks et al., suggesting that DAMN might be a key intermediate in the photochemically activated synthesis of nucleobases from formamide.[10] In addition, our quantum chemical calculations have shown that there exists an exergonic reaction pathway that connects formamide to diaminomaleonitrile if free CN· radicals are present in the reaction mixture. This reaction mechanism is entirely new and leads to the formation of DAMN via AHAN and AHMN, i.e. via intermediates, which have been proposed to participate in the nonphotochemical HCN-based synthesis of nucleobases.[50]

ASSOCIATED CONTENT

Supporting Information

Optimized geometries and computed total energies of all structures considered in this study. This material is available free of charge via the Internet at http://pubs.acs.org.

AUTHOR INFORMATION

Corresponding Author

judit@ncbr.muni.cz; svatopluk.civis@jh-inst.cas.cz

Notes

The authors declare no competing financial interest.

ACKNOWLEDGMENTS

The authors gratefully acknowledge financial support from the Grant Agency of the Czech Republic (Grant No. P208/10/2302), from the project "CEITEC—Central European Institute of Technology" (CZ.1.05/1.1.00/02.0068) from the European Regional Development Fund, from the Grant Agency of the Academy of Sciences of the Czech Republic (Grant No. IAAX00100903), and the Ministry of Education, Youth, and Sports of the Czech Republic (grant No. LM2010014).

REFERENCES

(1) Gibb, E. L.; Whittet, D. C. B.; Schutte, W. A.; Boogert, A. C. A.; Chiar, J. E.; Ehrenfreund, P.; Gerakines, P. A.; Keane, J. V.; Tielens, A.; van Dishoeck, E. F.; Kerkhof, O. *Astrophys. J.* **2000**, *536*, 347–356.

(2) Bockelee-Morvan, D.; Lis, D. C.; Wink, J. E.; Despois, D.; Crovisier, J.; Bachiller, R.; Benford, D. J.; Biver, N.; Colom, P.; Davies, J. K.; Gerard, E.; Germain, B.; Houde, M.; Mehringer, D.; Moreno, R.; Paubert, G.; Phillips, T. G.; Rauer, H. *Astron. Astrophys.* **2000**, *353*, 1101–1114.

(3) Saladino, R.; Crestini, C.; Ciciriello, F.; Costanzo, G.; Di Mauro, E. *Chem. Biodiversity* **2007**, *4*, 694–720.

(4) Yamada, H.; Okamoto, T. *Chem. Pharm. Bull.* **1972**, *20*, 623–624.

(5) Ochiai, M.; Marumoto, R.; Kobayashi, S.; Shimazu, H.; Morita, K. *Tetrahedron* **1968**, *24*, 5731–5737.

(6) Saladino, R.; Crestini, C.; Costanzo, G.; DiMauro, E. *Curr. Org. Chem.* **2004**, *8*, 1425–1443.

(7) Costanzo, G.; Saladino, R.; Crestini, C.; Ciciriello, F.; Di Mauro, E. *BMC Evol. Biol.* **2007**, *7* (Suppl 2), S1.

(8) Saladino, R.; Crestini, C.; Neri, V.; Ciciriello, F.; Costanzo, G.; Mauro, E. *ChemBioChem* **2006**, *7*, 1707–1714.

(9) Sponer, J. E.; Mladek, A.; Sponer, J.; Fuentes-Cabrera, M. *J. Phys. Chem. A* **2012**, *116*, 720–726.

(10) Barks, H. L.; Buckley, R.; Grieves, G. A.; Di Mauro, E.; Hud, N. V.; Orlando, T. M. *ChemBioChem* **2010**, *11*, 1240–1243.

(11) Saladino, R.; Brucato, J. R.; De Sio, A.; Botta, G.; Pace, E.; Gambicorti, L. *Astrobiology* **2011**, *11*, 815–824.

(12) Babankova, D.; Civis, S.; Juha, L. *Prog. Quantum Electron.* **2006**, *30*, 75–88.

(13) Civis, S.; Babankova, D.; Cihelka, J.; Sazama, P.; Juha, L. *J. Phys. Chem. A* **2008**, *112*, 7162–7169.

(14) Sovova, K.; Matulkova, I.; Kamas, M.; Dryahina, K.; Spanel, P.; Juha, L.; Civis, S. *Orig. Life Evol. Biospheres* **2009**, *39*, 249–250.

(15) Ferus, M.; Matulkova, I.; Juha, L.; Civis, S. *Chem. Phys. Lett.* **2009**, *472*, 14–18.

(16) Civis, S.; Juha, L.; Babankova, D.; Cvacka, J.; Frank, O.; Jehlicka, J.; Kralikova, B.; Krasa, J.; Kubat, P.; Muck, A.; Pfeifer, M.; Skala, J.; Ullschmied, J. *Chem. Phys. Lett.* **2004**, *386*, 169–173.

(17) Babankova, D.; Civis, S.; Juha, L.; Bittner, M.; Cihelka, J.; Pfeifer, M.; Skala, J.; Bartnik, A.; Fiedorowicz, H.; Mikolajczyk, J.; Ryc, L.; Sedivcova, T. *J. Phys. Chem. A* **2006**, *110*, 12113–12120.

(18) Ferus, M.; Kubelik, P.; Civis, S. *J. Phys. Chem. A* **2011**, *115*, 12132–12141.

(19) Civis, S.; Kubelik, P.; Ferus, M. *J. Phys. Chem. A* **2012**, *116*, 3137–3147.

(20) Ferus, M.; Kubelik, P.; Kawaguchi, K.; Dryahina, K.; Spanel, P.; Civis, S. *J. Phys. Chem. A* **2011**, *115*, 1885–1899.

(21) Mignon, P.; Sodupe, M. *Phys. Chem. Chem. Phys.* **2012**, *14*, 945–954.

(22) Mignon, P.; Ugliengo, P.; Sodupe, M. *J. Phys. Chem. C* **2009**, *113*, 13741–13749.

(23) Mignon, P.; Ugliengo, P.; Sodupe, M. *Orig. Life Evol. Biospheres* **2009**, *39*, 281–282.

(24) Mignon, P.; Ugliengo, P.; Sodupe, M.; Hernandez, E. R. *Phys. Chem. Chem. Phys.* **2010**, *12*, 688–697.

(25) Sponer, J. E.; Sponer, J.; Fuentes-Cabrera, M. *Chem.—Eur. J.* **2011**, *17*, 847–854.

(26) Sponer, J. E.; Sumpter, B. G.; Leszczynski, J.; Sponer, J.; Fuentes-Cabrera, M. *Chem.—Eur. J.* **2008**, *14*, 9990–9998.

(27) Sponer, J. E.; Vazquez-Mayagoitia, A.; Sumpter, B. G.; Leszczynski, J.; Sponer, J.; Otyepka, M.; Banas, P.; Fuentes-Cabrera, M. *Chem.—Eur. J.* **2010**, *16*, 3057–3065.

(28) Glaser, R.; Hodgen, B.; Farrelly, D.; McKee, E. *Astrobiology* **2007**, *7*, 455−470.
(29) Roy, D.; Najafian, K.; Schleyer, P. v. R. *Proc. Natl. Acad. Sci. U. S. A.* **2007**, *104*, 17272−17277.
(30) Gupta, V. P.; Rawat, P.; Singh, R. N.; Tandon, P. *Comput. Theor. Chem.* **2012**, *983*, 7−15.
(31) Rus, B.; Rohlena, K.; Skala, J.; Kralikova, B.; Jungwirth, K.; Ullschmied, J.; Witte, K. J.; Baumhacker, H. *Laser Part. Beams* **1999**, *17*, 179−194.
(32) Cassidy, W. A.; Villar, L. M.; Bunch, T. E.; Kohman, T. P.; Milton, D. J. *Science* **1965**, *149*, 1055−1064.
(33) Frisch, M. J.; Trucks, G. W.; Schlegel, H. B.; Scuseria, G. E.; Rob, M. A.; Cheeseman, J. R.; Montgomery, J. A., Jr.; Vreven, T.; Kudin, K. N.; Burant, J. C.; Millam, J. M.; Iyengar, S. S.; Tomasi, J.; Barone, V.; Mennucci, B.; Cossi, M.; Scalmani, G.; Rega, N.; Petersson, G. A.; Nakatsuji, H.; Hada, M.; Ehara, M.; Toyota, K.; Fukuda, R.; Hasegawa, J.; Ishida, M.; Nakajima, T.; Honda, Y.; Kitao, O.; Nakai, H.; Klene, M.; Li, X.; Knox, J. E.; Hratchian, H. P.; Cross, J. B.; Bakken, V.; Adamo, C.; Jaramillo, J.; Gomperts, R.; Stratmann, R. E.; Yazyev, O.; Austin, A. J.; Cammi, R.; Pomelli, C.; Ochterski, J. W.; Ayala, P. Y.; Morokuma, K.; Voth, G. A.; Salvador, P.; Dannenberg, J. J.; Zakrzewski, V. G.; Dapprich, S.; Daniels, A. D.; Strain, M. C.; Farkas, O.; Malick, D. K.; Rabuck, A. D.; Raghavachari, K.; Foresman, J. B.; Ortiz, J. V.; Cui, Q.; Baboul, A. G.; Clifford, S.; Cioslowski, J.; Stefanov, B. B.; Liu, G.; Liashenko, A.; Piskorz, P.; Komaromi, I.; Martin, R. L.; Fox, D. J.; Keith, T.; Al-Laham, M. A.; Peng, C. Y.; Nanayakkara, A.; Challacombe, M.; Gill, P. M. W.; Johnson, B.; Chen, W.; Wong, M. W.; Gonzalez, C.; Pople, J. A. *Gaussian 03*; Gaussian Inc.: Wallingford, CT, 2003.
(34) Eichkorn, K.; Treutler, O.; Ohm, H.; Haser, M.; Ahlrichs, R. *Chem. Phys. Lett.* **1995**, *240*, 283−289.
(35) Eichkorn, K.; Weigend, F.; Treutler, O.; Ahlrichs, R. *Theor. Chem. Acc.* **1997**, *97*, 119−124.
(36) Ahlrichs, R.; Bar, M.; Haser, M.; Horn, H.; Kolmel, C. *Chem. Phys. Lett.* **1989**, *162*, 165−169.
(37) McNaughton, D.; Evans, C. J.; Lane, S.; Nielsen, C. J. *J. Mol. Spectrosc.* **1999**, *193*, 104−117.
(38) (a) King, S.-T. *J. Phys. Chem.* **1971**, *75*, 405−410. (b) Hansen, E. L.; Larsen, N. W.; Nicolaisen, F. M. *Chem. Phys. Lett.* **1980**, *69*, 327−331. (c) Sugawara, Y.; Hamada, Y.; Tsuboi, M. *Bull. Chem. Soc. Jpn.* **1983**, *56*, 1045−1050.
(39) Kwiatkowski, J. S.; Leszczynski, J. *J. Mol. Struct.* **1993**, *297*, 277−284.
(40) Watson, T. M.; Hirst, J. D. *J. Phys. Chem. A* **2002**, *106*, 7858−7867.
(41) Papamokos, G. V.; Demetropoulos, I. N. *J. Phys. Chem. A* **2004**, *108*, 7291−7300.
(42) Mardyukov, A.; Sanchez-Garcia, E.; Rodziewicz, P.; Doltsinis, N. L.; Sander, W. *J. Phys. Chem. A* **2007**, *111*, 10552−10561.
(43) Buczek, A.; Kupka, T.; Broda, M. A. *J. Mol. Model.* **2011**, *17*, 2265−2274.
(44) Bende, A.; Suhai, S. *Int. J. Quantum Chem.* **2005**, *103*, 841−853.
(45) Sinha, P.; Boesch, S. E.; Gu, C. M.; Wheeler, R. A.; Wilson, A. K. *J. Phys. Chem. A* **2004**, *108*, 9213−9217.
(46) Vargas, R.; Garza, J.; Friesner, R. A.; Stern, H.; Hay, B. P.; Dixon, D. A. *J. Phys. Chem. A* **2001**, *105*, 4963−4968.
(47) Frey, J. A.; Leutwyler, S. *J. Phys. Chem. A* **2006**, *110*, 12512−12518.
(48) Heikkila, A. T.; Lundell, J. *J. Phys. Chem. A* **2000**, *104*, 6637−6643.
(49) Let us note that we have detected a large amount of $CN^{\bullet}$ radicals in the laser-induced dissociation of formamide.
(50) Hudson, J. S.; Eberle, J. F.; Vachhani, R. H.; Rogers, L. C.; Wade, J. H.; Krishnamurthy, R.; Springsteen, G. *Angew. Chem., Int. Ed.* **2012**, *51*, 5134−5137.
(51) Since this band is not observed in the spectra of our UV-irradiated samples, our results suggest that formation of a C−C bond between formamide and HCN requires a high energy impact event.